PHYSICAL REVIEW A VOLUME 50, NUMBER 6 DECEMBER 1994

Dependence of electron-impact dissociative excitation cross sections on the initial vibrational quantum number in H_2 and D_2 molecules: $X\,^1\Sigma_g^+ \rightarrow B\,^1\Sigma_u^+$ and $X\,^1\Sigma_g^+ \rightarrow C\,^1\Pi_u$ transitions

R. Celiberto, U. T. Lamanna, and M. Capitelli
Centro di Studio per la Chimica dei Plasmi del Consiglio Nazionale delle Ricerche, Bari, Italy
and Dipartimento di Chimica, Università di Bari, Bari, Italy

(Received 4 January 1994)

Electron-impact dissociative cross sections for H_2 and D_2 vibrationally excited molecules have been calculated in the frame of the impact-parameter method for dissociative processes involving direct dissociation $M_2(X\,^1\Sigma_g^+,v_i)+e\rightarrow M_2^*(B\,^1\Sigma_u^+,C\,^1\Pi_u)+e\rightarrow 2M+e$ and radiative cascade $M_2(X\,^1\Sigma_g^+,v_i)+e\rightarrow M_2^*(B\,^1\Sigma_u^+,C\,^1\Pi_u)+e\rightarrow M_2(X\,^1\Sigma_g^+)+e+h\nu\rightarrow 2M+e+h\nu$ (M_2 represents a hydrogen or deuterium molecule). The results show that direct dissociation cross sections strongly depend on the initial vibrational state of the molecule, while an opposite behavior is found in the case of dissociation by radiative cascade. Moreover, for this last process, the fraction of molecules that undergoes dissociation has been evaluated with respect to the total cascade process, yielding in general quite small values in both the H_2 and D_2 cases.

PACS number(s): 34.80.Gs, 52.20.Fs

I. INTRODUCTION

A lot of theoretical work has recently been devoted to the understanding of elementary processes responsible for the creation of H^- and D^- negative ions in multicusp magnetic plasma. Dissociative attachment from vibrationally excited molecules is the main process for formation of negative ions, and its efficiency, i.e., the production rate of H^- and D^-, strongly depends on the initial vibrational level of the molecules [1]. Therefore, all the elementary processes that can lead to the formation or destruction of vibrationally excited molecules or, in general, can affect the vibrational population, are of fundamental importance in the modeling of these kinds of plasmas [1].

One of the most important processes that occurs in the multicusp magnetic plasmas for populating the high vibrational states is the so-called radiative decay process (also known as the E-V process), i.e.,

$$\begin{array}{l} H_2(X\,^1\Sigma_g^+,v_i)+e\rightarrow H_2^*(\text{singlet states})+e \\ \qquad\qquad\searrow \\ \qquad\qquad\qquad H_2(X\,^1\Sigma_g^+,v_f)+h\nu\ , \end{array} \tag{1}$$

where the H_2 molecule, initially in the vibrational level v_i, excited by electron impact in a singlet electronic state decays radiatively in the manifold of v_f vibrational levels of the electronic ground state. This process has been extensively studied by Hiskes [2,3], and more recently by our group using excitation cross sections calculated according to the impact-parameter method [4,5].

On the other hand, the dissociation can be considered one of the main processes responsible for the destruction of vibrationally excited $H_2(v_i)$ molecules.

Although in general the excitation to the completely repulsive electronic state $b\,^3\Sigma_u^+$ is the main dissociative process [6], the dissociation can occur through many other important channels. In particular, in this paper, we will take into account the following processes induced by electron impact (involving either H_2 or D_2 molecules).

(a) Direct dissociation from electronically excited singlet states:

$$H_2(v_i)+e\rightarrow H_2^*+e\rightarrow H(n,l)+H(n',l')+e\ , \tag{2}$$

where H_2^* represents a molecule excited over the repulsive part of the bound potential curve of an excited singlet electronic state, and n,l and n',l' define the quantum state of H atoms.

(b) Dissociative decay:

$$\begin{array}{l} H_2(X\,^1\Sigma_g^+,v_i)+e\rightarrow H_2^*(\text{singlet state})+e \\ \qquad\qquad\searrow \\ \qquad\qquad\qquad H_2(X\,^1\Sigma_g^+,\varepsilon)+h\nu \\ \qquad\qquad\qquad\searrow \\ \qquad\qquad\qquad\qquad H(1s)+H(1s)\ . \end{array} \tag{3}$$

This process occurs through the same mechanism of process (1), but in this case the H_2^* molecule decays in the continuum of the vibrational energies ε belonging to $X\,^1\Sigma_g^+$ ground electronic state.

Due to their importance in many fields of physics, dissociative processes have been widely studied for both H_2 and D_2 molecules. Cross-section data are now available in the literature for a large spectrum of electronic transitions. On the other hand, a common feature shown by this kind of data is that they are generally referred to molecules in their ground vibrational state, while, to our knowledge, the study of electronic transitions by electron impact involving vibrationally excited H_2 and D_2 molecules [6–8] is particularly poor.

1050-2947/94/50(6)/4778(8)/$06.00

In this paper we present a complete set of dissociative cross sections for processes (2) and (3) for hydrogen and deuterium as a function of v_i, discussing in particular the electronic transitions $X\,{}^1\Sigma_g^+ \to B\,{}^1\Sigma_u^+$ and $X\,{}^1\Sigma_g^+ \to C\,{}^1\Pi_u$ which represent the main singlet-singlet excitations involved in the above radiative decay process [9]. This work follows that of Ref. [4] (hereafter referred to as I), where the total excitation cross sections have been calculated as a function of the initial vibrational quantum number for the same transitions and for both H_2 and D_2 molecules.

In Sec. II we illustrate the impact-parameter method [8,10] used in these calculations, while the results are discussed in Sec. III. Finally a brief summary is given in Sec. IV.

II. METHOD OF CALCULATION

A. Direct dissociation

We performed the dissociative cross-section calculation in the frame of the impact-parameter method as formulated in Ref. [8]. In this section we collect and briefly discuss the relevant formulas, referring to paper I for computational details.

The dissociative excitation cross section can be written in the frame of impact-parameter method [8] as

$$\sigma_{v_i}^{\alpha_i \to \alpha_f}(E) = \int_{\varepsilon_{\min}}^{\varepsilon_{\max}} d\varepsilon\, S_{v_i,\varepsilon}^{\alpha_i\alpha_f} D_{v_i,\rho_0,\varepsilon}^{\alpha_i\alpha_f}(E) \ , \tag{4}$$

where v_i is the initial vibrational quantum number, α_i and α_f represent the initial and final electronic states of the molecule, respectively, and E is the incident energy of the impinging electron. ε is the continuum energy of the α_f state ranging between the dissociation threshold energy $\varepsilon_{\min}$ and $\varepsilon_{\max}$ defined by

$$\varepsilon_{\max} = E + \varepsilon_{v_i}^{\alpha_i} \ , \tag{5}$$

where $\varepsilon_{v_i}^{\alpha_i}$ is the eigenvalue of the v_ith vibrational level belonging to the α_i electronic state.

The "structural factor" $S_{v_i,\varepsilon}^{\alpha_i\alpha_f}$ is defined by [4]

$$S_{v_i,\varepsilon}^{\alpha_i\alpha_f} = \frac{m^2e^2}{3g_i\hbar^4}(2-\delta_{\Lambda_f,0})(2-\delta_{\Lambda_i,0}) \times \left| \int_0^\infty dR\, \chi_\varepsilon^{\alpha_f}(R) M_{\Lambda_f,\Lambda_i}(R) \chi_{v_i}^{\alpha_i}(R) \right|^2 \ , \tag{6}$$

where $\chi_\varepsilon^{\alpha_f}(R)$ and $\chi_{v_i}^{\alpha_i}(R)$ are the continuum and bound vibrational wave functions, respectively, and $M_{\Lambda_f,\Lambda_i}(R)$ is the usual electronic dipole transition moment depending on the internuclear distance R. All other quantities appearing in Eq. (6) have been defined in paper I.

The "dynamical factor" $D_{v_i,\rho_0,\varepsilon}^{\alpha_i\alpha_f}(E)$ depends on the continuum energy via the transition energy $\Delta E_{v_i,\varepsilon}^{\alpha_i\alpha_f}$ defined by

$$\Delta E_{v_i,\varepsilon}^{\alpha_i\alpha_f} = \varepsilon - \varepsilon_{v_i}^{\alpha_i} \ . \tag{7}$$

ρ_0 is the usual cutoff parameter introduced in the impact-parameter method to avoid divergent cross sections. Its values for every vibrational level of the ground electronic state have been obtained by using Eqs. (18) and (19) of paper I, where $\bar{R}$ has been set equal to the internuclear distance corresponding to the absolute maximum in the vibrational wave function. Table I contains the ρ_0 values for $X \to B$ and $X \to C$ transitions for both H_2 and D_2 molecules and for $v_i = 0$, 5, and 10. The explicit expression for $D_{v_i,\rho_0,\varepsilon}^{\alpha_i\alpha_f}(E)$ is given in paper I with the transition energy expressed by (7).

TABLE I. Cutoff parameter ρ_0 (a.u.) for some values of the initial vibrational quantum number v_i.

Transition	Vibrational quantum number v_i	H_2	D_2
$X \to B$	0	1.87	1.87
	5	1.98	1.95
	10	2.15	2.03
$X \to C$	0	2.03	2.03
	5	2.27	2.23
	10	2.42	2.34

The vibrational wave functions have been calculated by solving the radial Schrödinger equation

$$\left[-\frac{\hbar^2}{2\mu}\frac{d^2}{dR^2} + V_\alpha(R) - \varepsilon_v^\alpha \right] \chi_v^\alpha(R) = 0 \ , \tag{8}$$

where μ is the reduced mass of the molecule, $V_\alpha(R)$ is the electronic potential for the α state, and ε_v^α is the vibrational energy. The vibrational wave function for bound states has been obtained by expanding $\chi_v^\alpha(R)$ in harmonic-oscillator eigenfunctions. The potential $V_\alpha(R)$ has been calculated for both H_2 and D_2 molecules by linear interpolation of the data of Ref. [11] for X, B, and C electronic states. Moreover, for the last two states we calculated some values above the dissociation threshold performing configuration-interaction calculations with a basis set of Cartesian Gaussian functions reported in paper I. The results are shown in Table II.

The continuum vibrational wave function has been calculated using a method briefly outlined in the Appendix. In this case, for the repulsive portion of $V_\alpha(R)$ potential we interpolated the data of Table II, and for short inter-

TABLE II. Transition energies as a function of internuclear distance for $X\,{}^1\Sigma_g^+ \to B\,{}^1\Sigma_u^+$ and $X\,{}^1\Sigma_g^+ \to C\,{}^1\Pi_u$ electronic transitions of H_2.

Transition	Internuclear distance (a.u.)	Transition energy (a.u.)
$X \to B$	0.5	0.1352
	0.7365	−0.3580
	0.9109	−0.5255
$X \to C$	0.7	−0.3049

nuclear distances ($R < 0.5$ a.u. for the B state and $R < 0.7$ a.u. for the C state) we used the functional form

$$V_\alpha(R)=\frac{Ae^{-BR}}{R}\ , \tag{9}$$

where constants A and B have been determined by fitting the available potential values at the smallest internuclear distances [8].

Expression (4) for the cross section has been obtained in the frame of adiabatic-nuclei approximation, considering the rotational levels as degenerate [8].

B. Dissociative decay

The cross section $\sigma_{v_i}^{\alpha_i\to\alpha_f\to\alpha_i}(E)$ for the $\alpha_i\to\alpha_f$ electronic transition induced by electron impact on a molecule initially in the vibrational state v_i and followed by radiative cascade in the continuum energy of α_i state is given by

$$\sigma_{v_i}^{\alpha_i\to\alpha_f\to\alpha_i}(E)=\sum_{v'}\sigma_{v_i,v'}^{\alpha_i\to\alpha_f}(E)\frac{\int_{\varepsilon_{\rm th}}^{E_{v'}}d\varepsilon\ A_{\alpha_f\to\alpha_i}(v',\varepsilon)}{\sum_{v}A_{\alpha_f\to\alpha_i}(v',v)+\int_{\varepsilon_{\rm th}}^{E_{v'}}d\varepsilon\ A_{\alpha_f\to\alpha_i}(v',\varepsilon)}\ , \tag{10}$$

where v' is the quantum number of the bound vibrational levels belonging to the α_f state, and ε is the continuum energy ranging between the dissociative threshold energy $\varepsilon_{\rm th}$ of the α_i state and the v'th eigenvalue $E_{v'}$ of the α_f state. $A_{\alpha_f\to\alpha_i}(v',v)$ and $A_{\alpha_f\to\alpha_i}(v',\varepsilon)$ are the well-known Einstein coefficients for the bound-bound and bound-continuum $\alpha_f\to\alpha_i$ transitions, respectively, while $\sigma_{v_i,v'}^{\alpha_i\to\alpha_f}(E)$ is the electron-impact excitation cross section for the bound-bound $\alpha_i\to\alpha_f$ transition. The sum on v in the denominator of Eq. (10) runs over the bound vibrational levels of the α_i state.

Using these definitions, we are now able to write the total cross section $\sigma_{v_i}^{\rm tot}(E)$ for process (3). Taking into account the excited states $B\ {}^1\Sigma_u^+$ and $C\ {}^1\Pi_u$ and neglecting all the other singlet states, we have

$$\sigma_{v_i}^{\rm tot}(E)=\sigma_{v_i}^{X\to B\to X}(E)+\sigma_{v_i}^{X\to C\to X}(E)\ . \tag{11}$$

In order to calculate the cross section by Eqs. (10) and (11) we evaluated the Einstein coefficients $A_{B\to X}(v',\varepsilon)$ and $A_{C\to X}(v',\varepsilon)$ for D_2 according to the equation [12]

$$A_{\alpha_f\to\alpha_i}(v',\varepsilon)=2.142\times10^{10}(E_{v'}-\varepsilon)^3G \times|\langle\chi_\varepsilon^{\alpha_i}|M_{\Lambda_f,\Lambda_i}(R)|\chi_v^{\alpha_f}\rangle|^2\ , \tag{12}$$

where G is the degeneracy factor. The other Einstein coefficients entering into Eq. (10) for both H_2 and D_2 transitions have been taken from Ref. [13]. $\sigma_{v_i,v'}^{X\to B}(E)$ and $\sigma_{v_i,v'}^{X\to C}(E)$ for bound-bound transitions have been calculated by using the following equation [see paper I: Eq. (13) and ff]:

$$\sigma_{v_i,v'}^{\alpha_i\to\alpha_f}(E)=S_{v_i,v'}^{\alpha_i\alpha_f}D_{v_i,\rho_0,v'}^{\alpha_i\alpha_f}(E)\ , \tag{13}$$

where all the symbols have the same meaning as in Eq. (4), the only exceptions being the structural and the dynamical factors which now depend on the v' discrete vibrational levels. From Eqs. (4) and (13) we can obtain the total excitation cross section $\sigma_{v_i}^{\alpha_i\to\alpha_f}(E)_{\rm tot}$ as

$$\sigma_{v_i}^{\alpha_i\to\alpha_f}(E)_{\rm tot}=\sum_{v'}S_{v_i,v'}^{\alpha_i\alpha_f}D_{v_i,\rho_0,v'}^{\alpha_i\alpha_f}(E)+\sigma_{v_i}^{\alpha_i\to\alpha_f}(E)\ . \tag{14}$$

The cross sections calculated by Eqs. (4) and (13) have

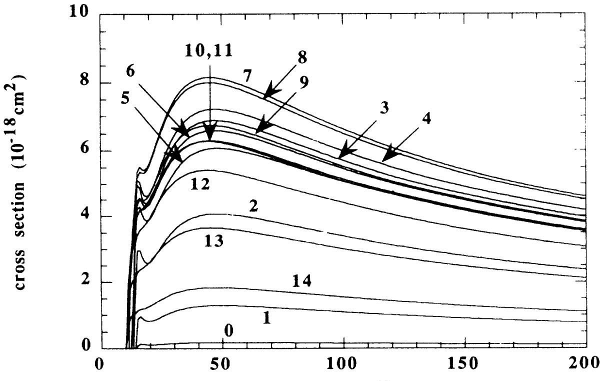

FIG. 1. Dissociative cross sections as a function of incident energy for the process $H_2(X\ {}^1\Sigma_g^+, v_i=0-14)+e\to H_2(B\ {}^1\Sigma_u^+)+e\to 2H+e$.

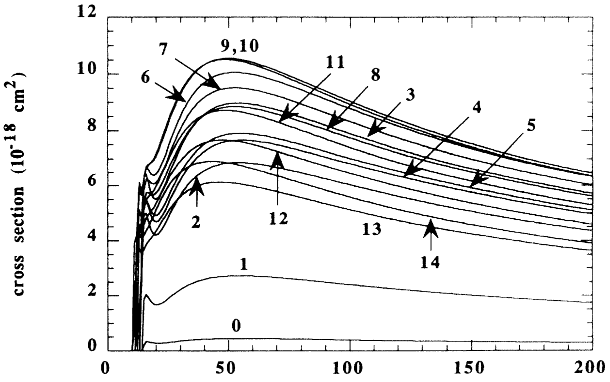

FIG. 2. Same as Fig. 1 for the process $H_2(X\ {}^1\Sigma_g^+, v_i=0-14)+e\to H_2(C\ {}^1\Pi_u)+e\to 2H+e$.

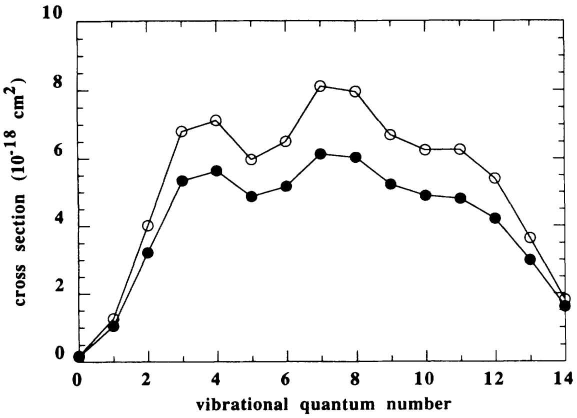

FIG. 3. Dissociative cross sections as a function of initial vibrational quantum number for the process $H_2(X\,^1\Sigma_g^+, v_i=0-14)+e \rightarrow H_2(B\,^1\Sigma_u^+)+e \rightarrow 2H+e$, with $E=40$ eV. Open circles: cross sections calculated by Eq. (4). Closed circles: cross sections calculated by Eq. (15).

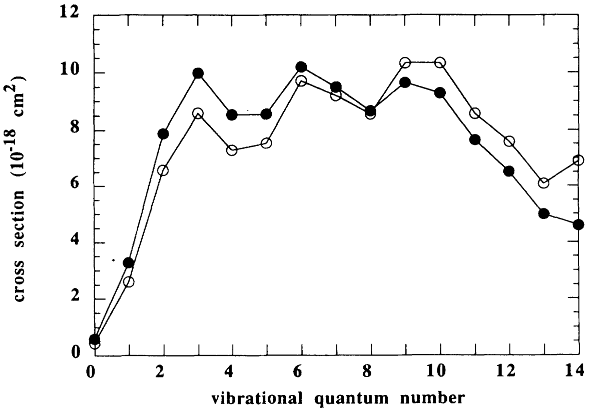

FIG. 5. Dissociative cross sections as a function of initial vibrational quantum number for the process $H_2(X\,^1\Sigma_g^+, v_i=0-14)+e \rightarrow H_2(C\,^1\Pi_u)+e \rightarrow 2H+e$, with $E=40$ eV. Open circles: cross sections calculated by Eq. (4). Closed circles: cross sections calculated in the Franck-Condon approximation [Eq. (16)].

been checked evaluating $\sigma_{v_i}^{\alpha_i \rightarrow \alpha_f}(E)_{\text{tot}}$ from Eq. (14): the results have been found to be in good agreement with the total cross sections reported in paper I.

III. RESULTS

A. Direct dissociation

In this section we will discuss the cross sections for the processes

$$H_2(X\,^1\Sigma_g^+, v_i)+e \rightarrow H_2^*(B\,^1\Sigma_u^+)+e \rightarrow H(1s)+H(2p)+e\ , \qquad \text{(a)}$$

$$H_2(X\,^1\Sigma_g^+, v_i)+e \rightarrow H_2^*(C\,^1\Pi_u)+e \rightarrow H(1s)+H(2p)+e\ , \qquad \text{(b)}$$

and corresponding ones for deuterium.

Figures 1 and 2 show the dissociative cross section for processes (a) and (b), respectively, as a function of incident energy for different initial vibrational quantum numbers ($0 \le v_i \le 14$). The intricate trend of the curves for different v_i values is mainly due to the overlap between the continuum and bound vibrational wave functions, respectively.

To better understand this point, we define a "modified" cross section

$$\sigma=\int_{\varepsilon_{\min}}^{\varepsilon_{\max}} d\varepsilon\, S_{v_i,\varepsilon}^{\alpha_i\alpha_f} \qquad (15)$$

obtained from Eq. (4) by artificially assuming the dynamical factor $D_{v_i,\rho_0,\varepsilon}^{\alpha_i\alpha_f}(E)$ is equal to 1. A comparison of the cross sections calculated by Eqs. (4) and (15) (see Figs. 3 and 4) clearly shows that the behavior of the two curves versus v_i is mainly determined by the structural factor $S_{v_i,\varepsilon}^{\alpha_i\alpha_f}$, which in turn depends on the vibrational wave function [see Eq. (6)]. Moreover Eq. (4) can be rearranged according to the Franck-Condon approximation as

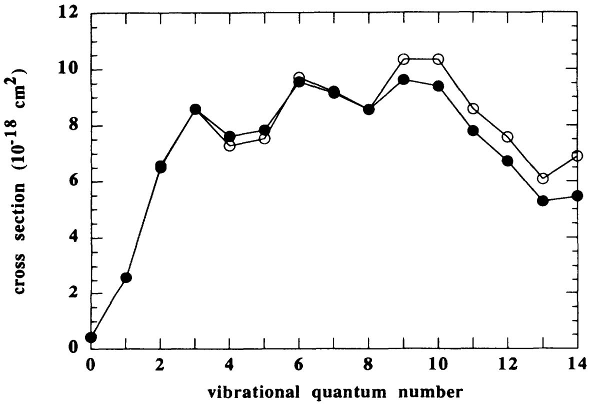

FIG. 4. Same as Fig. 3 for the process $H_2(X\,^1\Sigma_g^+, v_i=0-14)+e \rightarrow H_2(C\,^1\Pi_u)+e \rightarrow 2H+e$.

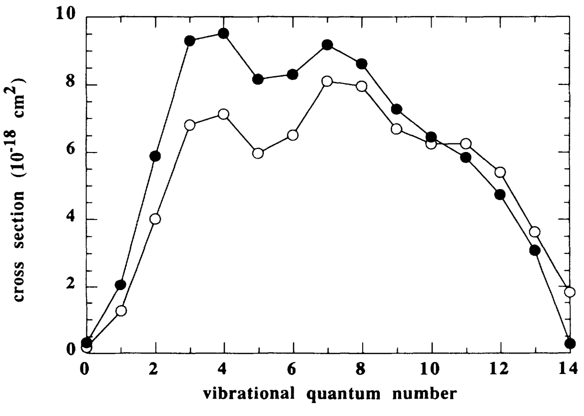

FIG. 6. Same as Fig. 5 for the process $H_2(X\,^1\Sigma_g^+, v_i=0-14)+e \rightarrow H_2(B\,^1\Sigma_u^+)+e \rightarrow 2H+e$.

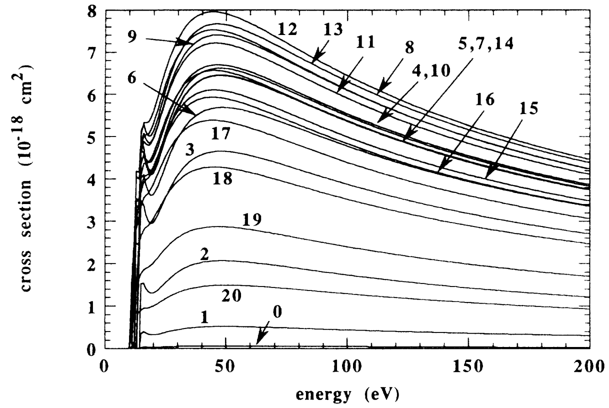

FIG. 7. Same as Fig. 1 for the process $D_2(X\,{}^1\Sigma_g^+, v_i=0\text{–}20) + e \rightarrow D_2(B\,{}^1\Sigma_u^+) + e \rightarrow 2D + e$.

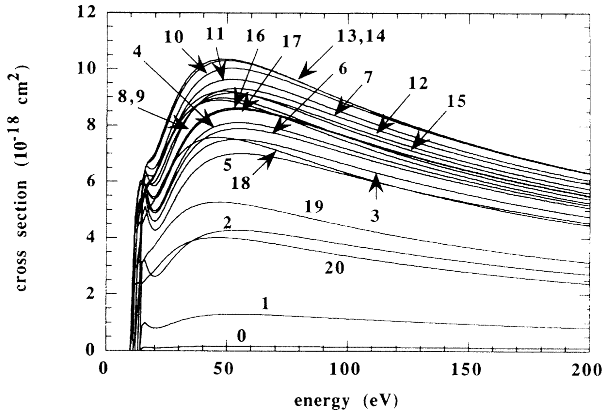

FIG. 8. Same as Fig. 1 for the process $D_2(X\,{}^1\Sigma_g^+, v_i=0\text{–}20) + e \rightarrow D_2(C\,{}^1\Pi_u) + e \rightarrow 2D + e$.

$$\sigma_{v_i}^{\alpha_i \rightarrow \alpha_f}(E)_{F-C} = \frac{m^2 e^2}{3 g_i \hbar^4}(2-\delta_{\Lambda_f,0})(2-\delta_{\Lambda_i,0})[M_{\Lambda_f,\Lambda_i}(R_{\text{eq}})]^2 \int_{\varepsilon_{\min}}^{\varepsilon_{\max}} d\varepsilon\, q_{v_i,\varepsilon} D_{v_i,\rho_0,\varepsilon}^{\alpha_i\alpha_f}(E) , \tag{16}$$

where R_{eq} is the ground-state equilibrium internuclear distance, and $q_{v_i,\varepsilon}$ is the well-known Franck-Condon density given by

$$q_{v_i,\varepsilon} = |\langle \chi_\varepsilon^{\alpha_f} | \chi_{v_i}^{\alpha_i} \rangle|^2 . \tag{17}$$

Again, inspection of Figs. 5 and 6, shows that the Franck-Condon approximation [Eq. (16)], closely follow the trend of the cross sections obtained by Eq. (4). This confirms that the cross-section behavior, as previously mentioned, depends mainly on the overlap integral of the vibrational wave functions appearing in the Franck-Condon density.

In Figs. 7 and 8 the dissociative cross sections as a function of incident energy involving $D_2(v_i)$ molecule for $X \rightarrow B$ and $X \rightarrow C$ transitions, respectively, are reported. One can note that the trend of cross sections in D_2 is similar to that observed for H_2. A comparison between H_2 and D_2 cross sections as a function of the initial vibrational quantum number for a fixed energy of 40 eV for both transitions is reported in Figs. 9 and 10. We can note an isotopic effect. In particular, the D_2 cross sections are shifted with respect to H_2 toward higher vibrational quantum numbers as a consequence of the lower vibrational energy of D_2 for the same v_i.

B. Dissociative decay

In Figs. 11 and 12 we report the cross sections for process (3) as a function of energy for hydrogen and deuterium, respectively. Both isotopes present a similar behavior. In particular the cross sections show large

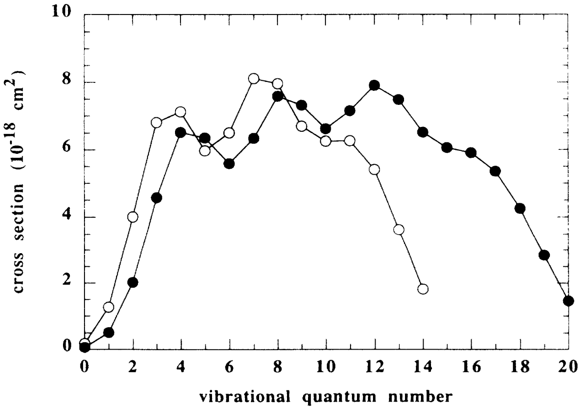

FIG. 9. Dissociative cross sections as a function of initial vibrational quantum number, with $E=40$ eV for the following processes: Open circles: $H_2(X\,{}^1\Sigma_g^+, v_i=0\text{–}14) + e \rightarrow H_2(B\,{}^1\Sigma_u^+) + e \rightarrow 2H + e$. closed circles: $D_2(X\,{}^1\Sigma_g^+, v_i=0\text{–}20) + e \rightarrow D_2(B\,{}^1\Sigma_u^+) + e \rightarrow 2D + e$.

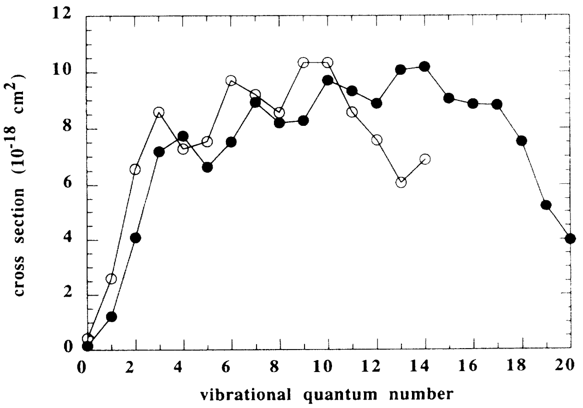

FIG. 10. Same as Fig. 9 for the processes Open circles: $H_2(X\,{}^1\Sigma_g^+, v_i=0\text{–}14) + e \rightarrow H_2(C\,{}^1\Pi_u) + e \rightarrow 2H + e$, closed circles: $D_2(X\,{}^1\Sigma_g^+, v_i=0\text{–}20) + e \rightarrow D_2(C\,{}^1\Pi_u) + e \rightarrow 2D + e$.

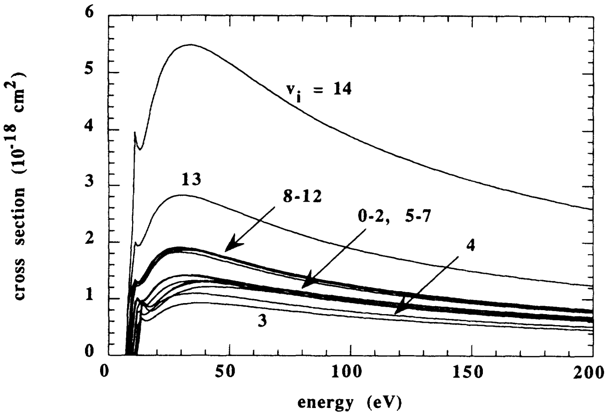

FIG. 11. Dissociative decay cross sections as a function of energy for the process $H_2(X\,^1\Sigma_g^+,v_i=0-14)+e \rightarrow H_2(B\,^1\Sigma_u^+,C\,^1\Pi_u)+e \rightarrow H_2(X\,^1\Sigma_g^+)+e+h\nu \rightarrow 2H(1s)+e+h\nu$.

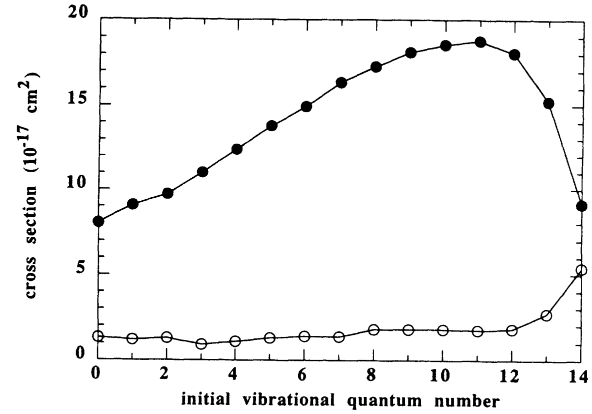

FIG. 13. Dissociative decay cross sections as a function of initial vibrational quantum number with $E=40$ eV for the processes $H_2(X\,^1\Sigma_g^+,v_i)+e \rightarrow H_2(B\,^1\Sigma_u^+,C\,^1\Pi_u)+e \rightarrow$ either $2H(1s)+e+h\nu$ (open circles) or $H_2(X\,^1\Sigma_g^+,v_f)+e+h\nu$ (closed circles).

values for very high quantum numbers ($v_i > 12$ for H_2 and $v_i > 18$ for D_2). This point can be better appreciated in Figs. 13 and 14, where the cross sections for process (3) and for a fixed incident energy of 40 eV are reported as a function of v_i. Except for the last v_i values, the cross sections show a weak dependence on the initial vibrational state of the molecule.

An interesting question arising in the study of these processes is the estimation of the fraction of molecules falling by cascade in the continuum part of the ground electronic state [2]. Actually, the major portion of the molecules collisionally excited in the B and C states repopulates by decaying the v_f discrete vibrational levels of the $X\,^1\Sigma_g^+$ state, while a small fraction undergoes dissociation following process (3). In order to evaluate the two contributions coming from process (1) (bound-to-bound) and dissociative process (3) (bound-to-continuum), in Figs. 13 and 14 we also report the cross sections for process (1), summed over all v_f final states [5] as a function of v_i. As aspected the bound-to-bound cross sections present values larger than the corresponding ones for the bound-to-continuum process, showing also a strong dependence on the initial vibrational quantum number. In Table III we report the ratio between the bound-to-continuum cross sections and the total cross sections (bound-to-bound plus bound-to-continuum) for $E=40$ eV for both H_2 and D_2 molecules as a function of v_i. This ratio in the case of H_2 does not exceed 15% for every v_i value, becoming quite a bit higher only for $v_i=14$. A similar behavior is observed in the D_2 case, so that no relevant isotopic effect is found in this kind of cross section.

IV. SUMMARY

In this paper we have presented a complete set of electron vibrationally excited H_2 and D_2 molecule cross sections for dissociative processes occurring through direct excitation of the dissociative part of electronically excited bound state, and through radiative cascade from the bound part of the same states. In the direct dissociation

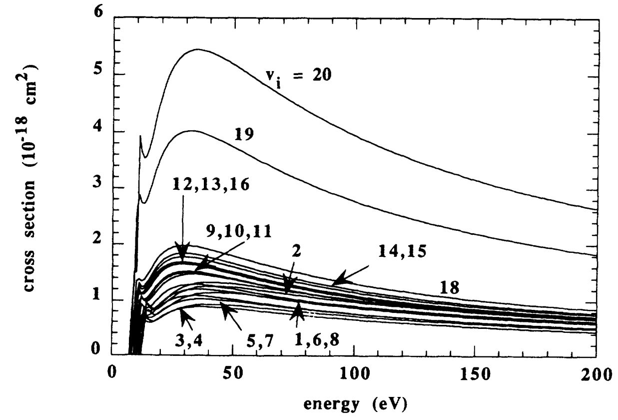

FIG. 12. Same as Fig. 11 for the process $D_2(X\,^1\Sigma_g^+,v_i=0-20)$ $+e \rightarrow D_2(B\,^1\Sigma_u^+,C\,^1\Pi_u)+e \rightarrow D_2(X\,^1\Sigma_g^+)$ $+e+h\nu \rightarrow 2D(1s)+e+h\nu$.

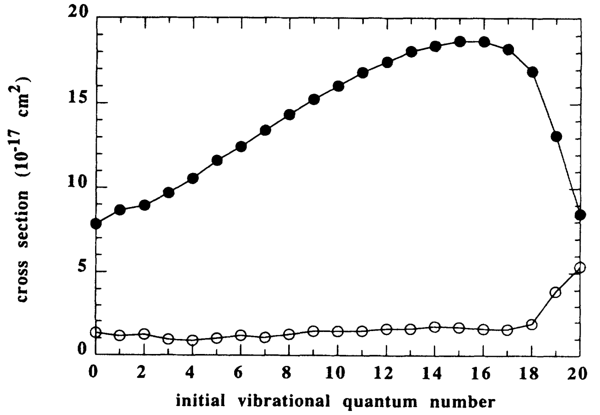

FIG. 14. Same as Fig. 13 for the processes $D_2(X\,^1\Sigma_g^+,v_i)$ $+e \rightarrow D_2(B\,^1\Sigma_u^+,C\,^1\Pi_u)+e \rightarrow$ either $2D(1s)+e+h\nu$ (open circles) or $D_2(X\,^1\Sigma_g^+,v_f)+e+h\nu$ (closed circles).

TABLE III. Ratio of dissociative cross section to total cross section as a function of initial vibrational quantum number for $E=40$ eV for H_2 and D_2 molecules.

v_i	H_2 (%)	D_2 (%)
0	14	15
1	12	12
2	12	12
3	8	9
4	8	8
5	9	8
6	9	9
7	8	7
8	10	8
9	9	9
10	9	8
11	9	8
12	9	8
13	15	8
14	37	9
15		8
16		8
17		8
18		10
19		23
20		39

we found a strong and irregular dependence of the cross section on the vibrational quantum number, mainly due to the behavior of the vibrational wave functions, while in the dissociation by radiative decay the cross sections are not particularly affected by the initial vibrational state of the molecule. Moreover, for this last process the ratio of "dissociative cross section to total cross section" as a function of v_i ranges from 7 to 15%, becoming markedly larger in the case of the highest vibrational quantum number.

ACKNOWLEDGMENTS

This work has been partially supported by "Progetto Finalizzato Chimica Fine" del CNR, by Ministero Università e Ricerca Scientifica e Technologica, as well as by Network EBRCHRXCT920003 "Negative ion production by volume and surface processes in plasmas."

APPENDIX

Equation (8) for the continuum vibrational states is written as

$$\left[\frac{-\hbar^2}{2\mu}\frac{d^2}{dR^2}+V_\alpha(R)-\varepsilon\right]\chi_\varepsilon^\alpha(R)=0\ , \tag{A1}$$

where ε is the continuum energy of the α electronic state.

The boundary conditions are given by

$$\chi_\varepsilon^\alpha(R)\rightarrow\begin{cases}0 \quad \text{for } R\rightarrow 0 & \text{(A2)}\\ A\sin(kR+\eta) \quad \text{for } R\rightarrow\infty\ , & \text{(A3)}\end{cases}$$

where η is the phase shift, A is a normalization constant given by [14]

$$A=\left[\frac{2\mu}{\hbar^2\pi k}\right]^{1/2}\ , \tag{A4}$$

and k is defined as

$$k^2=\frac{2\mu[\varepsilon-V_\alpha(R=\infty)]}{\hbar^2}\ . \tag{A5}$$

Due to the formal analogy of Eq. (A1) with the scattering equations, we can approach its solution by using the same numerical methods developed in the scattering theory [15]. We may start transforming Eq. (A1), in the frame of the Green's-function formalism, in integral form [16]:

$$\chi_\varepsilon^\alpha(R)=C\sin(kR)-\frac{\cos(kR)}{k}\int_0^R dR'\sin(kR')U_\alpha(R')\chi_\varepsilon^\alpha(R')-\frac{\sin(kR)}{k}\int_R^\infty dR'\cos(kR')U_\alpha(R')\chi_\varepsilon^\alpha(R')\ , \tag{A6}$$

where $U_\alpha(R)=(2\mu/\hbar^2)V_\alpha(R)$, and C is a normalization constant.

Adding and subtracting the following quantity:

$$\frac{\sin(kR)}{k}\int_0^R dR'\cos(kR')U_\alpha(R')\chi_\varepsilon^\alpha(R')\ , \tag{A7}$$

Eq. (A6) becomes

$$\chi_\varepsilon^\alpha(R)=BC\sin(kR)-\frac{\cos(kR)}{k}\int_0^R dR'\sin(kR')U_\alpha(R')\chi_\varepsilon^\alpha(R')+\frac{\sin(kR)}{k}\int_0^R dR'\cos(kR')U_\alpha(R')\chi_\varepsilon^\alpha(R')\ , \tag{A8}$$

where the B factor is given by

$$B=1-\frac{1}{Ck}\int_0^\infty dR'\cos(kR')U_\alpha(R')\chi_\varepsilon^\alpha(R')\ . \tag{A9}$$

Defining the new function $u_\varepsilon^\alpha(R)$ as

$$\chi_\varepsilon^\alpha(R)=BCu_\varepsilon^\alpha(R)\ , \tag{A10}$$

we find from Eq. (A8) that

$$u_\varepsilon^\alpha(R)=\sin(kR)-\frac{\cos(kR)}{k}\int_0^R dR'\sin(kR')U_\alpha(R')u_\varepsilon^\alpha(R')+\frac{\sin(kR)}{k}\int_0^R dR'\cos(kR')U_\alpha(R')u_\varepsilon^\alpha(R') . \qquad \text{(A11)}$$

This equation can be resolved numerically in the simplest way by dividing the interval $\{0,R\}$ in a suitable grid of N mesh points separated by a constant increment ΔR, and using the trapezoidal rule to calculate the two integrals in the right-hand side. Thus

$$\begin{aligned} u_\varepsilon^\alpha(N\Delta R)=\sin(kN\Delta R)&-\frac{\cos(kN\Delta R)}{k}\sum_{i=0}^{N-1}\Delta R\,\sin(ki\Delta R)U_\alpha(i\Delta R)u_\varepsilon^\alpha(i\Delta R)\\ &+\frac{\sin(kN\Delta R)}{k}\sum_{i=0}^{N-1}\Delta R\,\cos(ki\Delta R)U_\alpha(i\Delta R)u_\varepsilon^\alpha(i\Delta R) . \end{aligned} \qquad \text{(A12)}$$

Since the Nth terms cancel each other, the two sums run over the range 0 to $N-1$, so that the function $u_\varepsilon^\alpha(N\Delta R)$ is related to its preceding N values.

The integration starts with the initial condition

$$u_\varepsilon^\alpha(0)=0 ,$$

and it is propagated up to the asymptotic region where the process can be stopped for a suitable R value where $U_\alpha(R)$ is sufficiently small.

Knowing the function $u_\varepsilon^\alpha(R)$ in all the mesh points, we can calculate the B factor from Eqs. (A9) and (A10):

$$B=\frac{1}{1+\frac{1}{k}\int_0^\infty dR'\cos(kR')U_\alpha(R')u_\varepsilon^\alpha(R')} . \qquad \text{(A13)}$$

The normalization constant C is found by comparison between the boundary condition (A3), rewritten as

$$\chi_\varepsilon^\alpha(R')\to A\cos(\eta)\{\sin(kR)+\tan(\eta)\cos(kR)\} \quad \text{for } R\to\infty , \qquad \text{(A14)}$$

and the asymptotic form of Eq. (A6):

$$\chi_\varepsilon^\alpha(R)=C\sin(kR) -\frac{\cos(kR)}{k}\int_0^\infty dR'\sin(kR')U_\alpha(R')\chi_\varepsilon^\alpha(R') . \qquad \text{(A15)}$$

Using Eq. (A10) it is easy to show that

$$C=A\cos(\eta) , \qquad \text{(A16)}$$

$$\tan(\eta)=-\frac{B}{k}\int_0^\infty dR\,\sin(kR)U_\alpha(R)u_\varepsilon^\alpha(R) . \qquad \text{(A17)}$$

Finally, $\chi_\varepsilon^\alpha(R)$ is calculated from Eq. (A10).

[1] C. Gorse, R. Celiberto, M. Cacciatore, A. Laganà, and M. Capitelli, Chem. Phys. **161**, 211 (1992).

[2] J. R. Hiskes, J. Appl. Phys. **51**, 4592 (1980).

[3] J. R. Hiskes, J. Appl. Phys. **70**, 3409 (1991).

[4] R. Celiberto and T. N. Rescigno, Phys. Rev. A **47**, 1939 (1993).

[5] R. Celiberto, M. Capitelli, and U. T. Lamanna, Chem. Phys. **183**, 101 (1994).

[6] R. Celiberto, M. Cacciatore, M. Capitelli, and C. Gorse, Chem. Phys. **133**, 355 (1989); R. Celiberto, M. Cacciatore and M. Capitelli, *ibid.* **133**, 369 (1989).

[7] T. N. Rescigno and B. I. Schneider, J. Phys. B **21**, L691 (1988).

[8] M. J. Redmon, B. C. Garret, L. T. Redmon, and C. W. McCurdy, Phys. Rev. A **32**, 3354 (1985).

[9] J. R. Hiskes, Comments At. Mol. Phys. **19**, 59 (1987).

[10] A. U. Hazi, Phys. Rev. A **23**, 2232 (1981).

[11] W. Kolos and L. Wolniewicz, J. Chem. Phys. **43**, 2429 (1965); W. Kolos and L. Wolniewicz, *ibid*, **48**, 3672 (1968); L. Wolniewicz, *ibid.*, **51**, 5002 (1969).

[12] M. Glass-Maujean, At. Data Nucl. Data Tables **30** 301 (1984).

[13] T. L. Stephens and A. Dalgarno, J. Quantum Spectrosc. Radiat. Transfer **12**, 569 (1972); A. C. Allison and A. Dalgarno, At. Data **1**, 289 (1970).

[14] S. Chung and C. Lin, Phys. Rev. A **12**, 1340 (1975).

[15] L. D. Thomas, J. Comput. Phys. **13**, 348 (1973).

[16] L. S. Rodberg and R. M. Thaler, *Introduction to Quantum Theory of Scattering* (Academic, New York, 1967).